

Modeling and Simulation of Skeletal Muscle for Computer Graphics: A Survey

By Dongwoon Lee, Michael Glueck, Azam Khan,
Eugene Fiume and Ken Jackson

Contents

1 Introduction	230
2 Background	233
2.1 Structural Description	234
2.2 Muscle Architecture	235
2.3 Muscle Contraction	236
2.4 Mechanical Properties	237
2.5 Mechanical Models	239
2.6 Limitations of Mechanical Models	241
3 Muscle Deformation	243
3.1 Geometrically-Based Approaches	243
3.2 Physically-Based Approaches	247
3.3 Data-Driven Approaches	254
4 Control and Simulation	258
4.1 Static Optimization	260
4.2 Dynamic Optimization	263

5 Discussion and Conclusion	265
Acknowledgements	269
References	270

Modeling and Simulation of Skeletal Muscle for Computer Graphics: A Survey

Dongwoon Lee¹, Michael Glueck², Azam Khan³,
Eugene Fiume⁴ and Ken Jackson⁵

¹ *Autodesk Research, Canada and University of Toronto, Canada,
dwlee@cs.toronto.edu*

² *Autodesk Research, Canada, Michael.Glueck@autodesk.com*

³ *Autodesk Research, Canada, Azam.Khan@autodesk.com*

⁴ *University of Toronto, Canada, elf@dgp.toronto.edu*

⁵ *University of Toronto, Canada, krj@cs.toronto.edu*

Abstract

Muscles provide physiological functions to drive body movement and anatomically characterize body shape, making them a crucial component of modeling animated human figures. Substantial effort has been devoted to developing computational models of muscles for the purpose of increasing realism and accuracy in computer graphics and biomechanics. We survey various approaches to model and simulate muscles both morphologically and functionally. Modeling the realistic morphology of muscle requires that muscle deformation be accurately depicted. To this end, several methodologies are presented, including geometrically-based, physically-based, and data-driven approaches. On the other hand, the simulation of physiological muscle functions aims to identify the biomechanical controls responsible for realistic human motion. Estimating these muscle controls has been pursued through static and dynamic simulations. We review and discuss all these approaches, and conclude with suggestions for future research.

1

Introduction

Computational human modeling has been an important research topic in many domains: from films and video games, to augmented and virtual reality, in which virtual humans play vital roles. As the value of virtual human models extends to new areas, such as ergonomics, medicine, and biomechanics, there is a rapidly growing need for and interest in modeling humans stemming from these new applications. Different approaches to modeling humans address different performance requirements. For example, while greater interactivity is required for real-time applications, greater visual realism is more desirable in film production. Moreover, physiological and biomechanical accuracy are the most crucial in designing medical applications. Despite considerable effort, the immense complexity of the human body continues to make modeling it computationally extremely challenging. Furthermore, our keen perception of human bodies and their movement can make us very critical of even small deviations from expected behavior.

The human body is composed of an intricate and complex anatomical structure which is made up of a variety of interacting tissues. Computational human modeling requires accurate reconstruction of this anatomical structure, the relevant biological and physiological

functions, and their mathematical formulation into practical physical and mechanical models. Among the various tissues composing the body, those that form muscles carry out diverse physiological functions and collectively perform body movement. This survey focuses specifically on skeletal muscles because they impart two important features essential for computational human modeling. First, skeletal muscles serve as major body components which make up nearly 50% of total body weight, characterizing the shape of a body and its tone. Second, they provide physiological functions to stabilize body posture and drive body movement. While the former is a key feature for realistic representation of the body which demands accurate modeling of muscle morphology, the latter is crucial for realistic animation of body movement which needs accurate simulation of muscle functions.

Early approaches [11, 52] proposed human models based on rigid skeletons. While they have been widely used in various biomechanical studies, such as biped locomotion analysis, their capacity is fairly limited to represent the human body realistically and they have difficulties in modeling soft tissues. Later, muscle and fatty tissue were introduced as additional layers to represent elastic deformation of soft bodies [17]. However, this muscle model is physically unrealistic and its application is limited to expressing bulging effects over joints. Various researchers thus devoted significant effort to developing realistic muscle models, focusing on accurate representation of muscle shape and its deformable behaviors. For example, anatomical knowledge has been integrated into constructing muscle geometry [10, 57, 69, 89] and medical imaging techniques have been employed to enhance visual quality [59]. Once muscle geometry is constructed, its deformable behaviors during muscle contraction need to be described. To this end, a variety of approaches have been proposed: geometrically-based, physically-based, and data-driven approaches. In the biomechanics community, skeletal muscles have also been extensively studied, but most of this review has focused on understanding their mechanical properties and physiological functions for human locomotion. As biomechanical models have been validated through rigorous experiments [34, 95], they have begun to draw the attention of graphics researchers, who study simulation of human motions based on computed muscle controls [41, 43, 44, 84], in

the hope of producing realistic human animation. In this survey, we examine and discuss these approaches with respect to two principal features of muscle: muscle deformation and muscle simulation.

This review is organized as follows. Section 2 gives a brief introduction to anatomical and biomechanical descriptions of muscle, which have been considered in most applications. In Section 3, we examine various approaches proposed to model muscle deformation. In Section 4, we address muscle control problems and present related simulation models to solve them. Section 5 concludes with a discussion of possible approaches to bridge the efforts of the biomechanical and graphics research communities, working toward a unified model.

2

Background

Muscles are the active tissues in the body that generate forces to drive motion. Depending on their physiological functions, muscles can be classified into three types: cardiac, smooth, and skeletal muscle. Cardiac muscles make up the walls of the heart, while smooth muscles constitute the walls of other organs or blood vessels. Both of these classes of muscle are controlled by the autonomic nervous system and contract without conscious effort. Unlike the first two classes of muscle, skeletal muscle contraction is controlled through the somatic nervous system and, for the most part, is done so consciously. These voluntary contractions produce forces that are transferred to the underlying skeleton, resulting in human body movement. Most research in graphics and related fields, such as biomechanics and robotics, has focused on understanding the physiological features and functions of skeletal muscles. In this section, we briefly review both anatomical and biomechanical aspects of skeletal muscle.

during locomotion, providing additional stability (e.g., the Achilles tendon during a human stride).

2.2 Muscle Architecture

Muscle architecture refers to the internal arrangement of fascicles within a muscle. Some muscles have simple architectures, in which the fascicles are arranged parallel to one another along the length of the muscle. These are typically the larger muscles, such as the *biceps brachii* or the *sartorius*. However, most muscles exhibit fascicles with an angular orientation, called the *pennation* angle, between their tendinous attachments and the longitudinal axis of the muscle. Muscles with angular fascicle arrangements are known as *pennate* muscles. Several types of pennation patterns are observed in skeletal muscles, as illustrated in Figure 2.2. Parallel muscles can have either longitudinally arranged fibers (e.g., *sartorius*) or similarly oriented fibers with tapering ends (e.g., *biceps brachii* and *psoas major*). Unipennate muscles have fibers arranged in a diagonal pattern to one side of tendon (e.g., *lumbricals* and *extensor digitorum longus*). Bipennate muscles have two rows of fibers, running in opposite diagonal directions on both sides of a central tendon (e.g., *rectus femoris*). Multipennate muscles have multiple rows of diagonal fibers, with a central tendon that branches into two or more tendons (e.g., *deltoid*). Convergent muscles have wider origin and narrower insertion (e.g., *pectoralis major*). These differences in muscle architecture determine the range of movement and power produced by a muscle. A muscle would contain a greater number of shorter muscle fibers in a pennate configuration than in a parallel configuration.

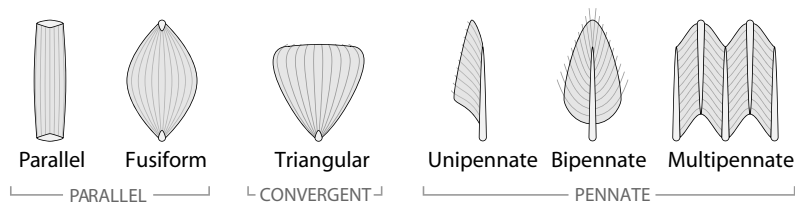


Fig. 2.2 Exemplary muscle architecture types. (Adapted from Ng-Thow-Hing [58].)

As such, pennate muscles do not shorten as much, but can produce more force than parallel muscles of the same size.

2.3 Muscle Contraction

Muscle contraction is controlled by the central nervous system; nerve impulses originate from and travel down the motor neurons to the sensory-somatic branch in the muscle. The place at which the terminal of a motor neuron and a muscle fiber connect is called the neuromuscular junction. Each motor neuron innervates a set of muscle fibers in which the nerve impulses stimulate the flow of calcium into the sarcomeres, causing their filaments to slide [37]. Sarcomeres have protein-based structures composed of high-tensile “thin” filaments of *actin* and “thick” filaments of *myosin*. They are alternately stacked on one another and interact via cross-bridges to produce force. The sliding filament and cross-bridge theory [34, 35] describes the process of muscle contraction. During muscle contraction, the lengths of these filaments remain constant and slide past each other to increase their overlap, producing an overall shortening effect in the muscle, as illustrated in Figure 2.3. The myosin heads are considered to be elastic elements which oscillate about an equilibrium position (i.e., position of attachment to the myosin filament) due to biochemical energy. They are linked as the cross-bridges to the myosin binding sites located in the actin filament. When the heads oscillate, they continuously attach or detach from the myosin binding site. When they attach, they exert forces on the actin filaments, causing filaments to slide past each other. Muscle contraction can be classified according to length change or force level. In *isotonic* contraction, muscle length changes while producing force;

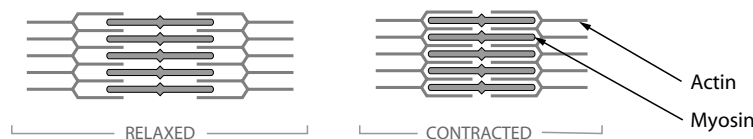


Fig. 2.3 During concentric muscle contraction, the sarcomere shortens as filaments of myosin pull along the rigid filaments of actin. The more the filaments overlaps, the more the sarcomere thickens. (Adapted from [37].)

the muscle either shortens (i.e., *concentric* contraction) or lengthens (i.e., *eccentric* contraction) depending on whether the produced force is sufficient to resist an external load. In *isometric* contraction, muscle length remains unchanged while producing force, as, for example, when holding up an object without moving.

2.4 Mechanical Properties

Mechanical properties of muscle associated with force development can be obtained from simple experiments using muscle isolated from tendon [26]. Two fundamental functional properties, with force-length and force-velocity, have been frequently incorporated into a variety of biomechanical models to study muscle function.

When the whole muscle is stretched or shortened to several different lengths (force-length property), the resulting force output is measured and plotted against the length. With no muscle activation, muscle only develops passive restorative force against increased stretching. With muscle activation, muscle contracts and generates active force. The total force is the sum of both active and passive forces (see Figure 2.4(a)). The curves for these forces are approximated in various

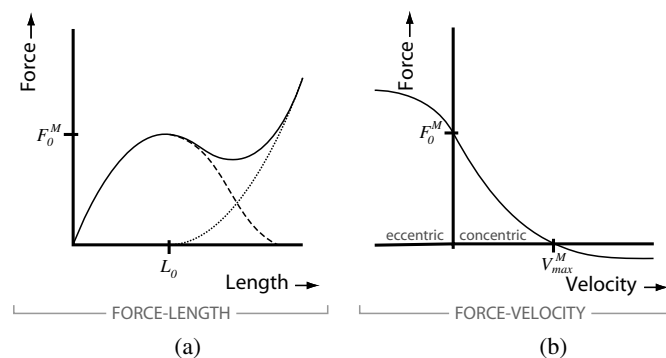


Fig. 2.4 Mechanical properties of muscles associated with force development. (Adapted from [95].) (a) A sample force-length plot shows the passive elastic (dotted), active (dashed), and total (solid) force generated by a muscle against its length. F_0^M is the maximum isometric force and L_0 is the rest/optimal length. F_0^M is experienced at L_0 . (b) A sample force-velocity plot shows the changes in force a muscle generates against the velocity of muscle contraction. V_{max}^M is the maximum shortening velocity.

ways, such as piecewise line segments [95], piecewise cubic spline [18] or quadratic functions [87]. The active force is found by subtracting the passive force from the total force. The nonlinear force-length relationship is consistent with the sliding filament theory of muscle contraction.

The force-velocity property of muscle is the relationship between the velocity at which muscle shortens and the amount of force it produces (plotted in Figure 2.4(b)). To quantify this relationship, a fully activated muscle is clamped isometrically and then suddenly released to allow shortening against an external load. When there is no load on the muscle, the maximum velocity of shortening is experienced. As the external load increases, the velocity of shortening decreases. The curve for this property is modeled by following hyperbolic equation (which is also known as the Hill equation) [31]:

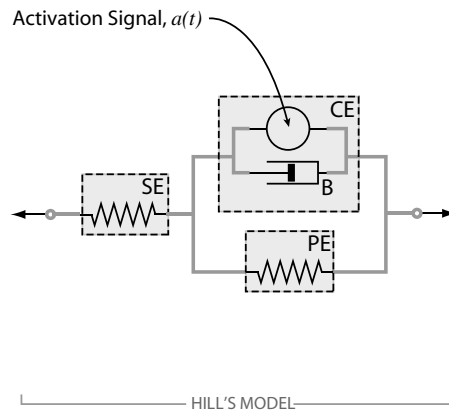
$$(F + a)(v + b) = (F_0 + a)/b, \quad (2.1)$$

where F is the force generated by muscle, v is the velocity of shortening, F_0 is the maximum isometric force, a and b are constants related to a specific class of muscle. This property is arguably thought to be associated with the dependence of muscle force on the number of attached cross-bridges [37]. During muscle contraction, cross-bridges attach to produce forces. Since it takes some amount of time for them to attach, as filaments slide past one another more quickly (i.e., muscle shortens with increasing velocity), the produced force decreases due to the lower number of attached cross-bridges. Conversely, as the relative velocity of filaments decreases (i.e., muscle shortens with decreasing velocity), more cross-bridges can take time to attach, producing more force.

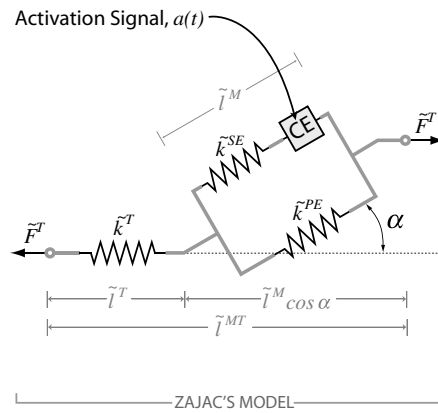
Another important property of muscle is *line of action*, which determines mechanical constraints on the behavior of muscle. There are two common methods to represent the line of action: piecewise line segments [22] and centroid curves [36]. Piecewise line segments specify the path of muscles to tendinous attachments. They can be wrapped around the joints or pass through the tendon sheaths. Centroid curves are constructed by interpolating approximate centroids of cross-sections throughout the muscle.

2.5 Mechanical Models

A simple and phenomenological mechanical model (shown in Figure 2.5(a)) was suggested by Gasser and Hill [26] to capture the mechanical properties of muscle discussed above. This model has three major components: the series element (SE), the parallel element (PE),



(a)



(b)

Fig. 2.5 Mechanical muscle models. (Adapted from Chen and Zeltzer [18].) (a) Hill's model describes the force of a muscle contracting as the sum of four elements: the contractile element (CE), the series elastic element (SE), the parallel element (PE) and the viscous element (B) that depends on the shortening velocity. (b) Zajac's model extends Hill's model, adding the pennation angle, α , of a muscle fiber.

and the contractile element (CE). The series element (SE) represents mainly the elastic effects of tendon and intrinsic elasticity within the sarcomere. The parallel element (PE) represents the passive elasticity of the muscle resulting from the penetration of connective tissues into the muscle body. The CE accounts for generation of active force that is dependent on the muscle length, l^M , and the time-varying neural signal, $a(t)$, originating from the central nervous system. The Hill model was later refined by Zajac [95] to be a dimensionless aggregate or “lumped” model that can be scaled easily to represent any skeletal musculotendon unit. The force components are modeled from the measurement of isolated muscle fibers, which directly reflect the nonlinear properties due to the sliding filaments. While the series elastic element can be lumped with the tendon and removed from the model, pennation effects are directly included into the model. In Zajac’s model, muscle length, l^M , tendon length, l^T , muscle force, F^M , and shortening velocity, v^M , are respectively normalized as

$$\tilde{l}^M = \frac{l^M}{l_0^M}, \quad \tilde{l}^T = \frac{l^T}{l_s^T}, \quad \tilde{F}^M = \frac{F^M}{F_0^M}, \quad \tilde{v}^M = \frac{v^M}{v_{\max}^M},$$

where l_0^M is optimal muscle length at which F_0^M is developed, l_s^T is tendon rest length, F_0^M is the maximum isometric force of active muscle, and v_{\max}^M is the maximum shortening velocity of muscle fibers. The relationship between muscle and musculotendon length is

$$\tilde{l}^{MT} = \tilde{l}^T + \tilde{l}^M \cos \alpha,$$

where α is the pennation angle (see Figure 2.5(b)). The normalized active force $\tilde{F}_{\text{active}}^{CE}$ and passive force \tilde{F}^{PE} can be approximated from the characteristic curves of force-length and force-velocity (shown in Figure 2.4). The production of contractile force \tilde{F}^{CE} is the $\tilde{F}_{\text{active}}^{CE}$ scaled by activation level, $a(t)$ varying with time t , and force-velocity relation, $F_v(\tilde{v}^M)$:

$$\tilde{F}^{CE} = a(t)F_v(\tilde{v}^M)\tilde{F}_{\text{active}}^{CE}(\tilde{l}^M)$$

Finally, the total force generated by the whole musculotendon unit is

$$\tilde{F}_M = (\tilde{F}^{CE} + \tilde{F}^{PE}) \cos \alpha. \quad (2.2)$$

Another commonly used muscle model is the Huxley model [34] which combines the sliding filaments and cross-bridge theory we reviewed in Section 2.3. While the Hill model has been used to describe macroscopic behaviors of muscle, the Huxley model has been used mainly to understand the properties of the microscopic contractile elements. To describe muscle contraction, the actin-myosin bonding reaction is expressed using first order kinetics as

$$\frac{dn}{dt} = \frac{\partial n}{\partial t} - v(t) \frac{\partial n}{\partial x} = (1 - n)f(x) - ng(x). \quad (2.3)$$

Here, the function $n(x, t)$ is proportional to the number of attached cross-bridges with displacement x at time t , $v(t)$ is the velocity of contraction of a half sarcomere, $f(x)$ is the rate of attachment, and $g(x)$ is the rate of detachment. The displacement x is the distance between the equilibrium position and the myosin binding position located in the actin filament. The cross-bridge is defined as the cross-link between the myosin head and the myosin binding position and its behavior is modeled using a Hookean spring with spring constant k . The total force exerted by muscle is calculated by summing the forces contributed by each bonded cross-bridge as

$$F(t) = \frac{mkAs(t)}{2l} \int_{-\infty}^{\infty} xn(x, t)dx, \quad (2.4)$$

where m is the number of cross-bridges per unit volume, A is the cross-sectional area of the muscle, $s(t)$ is the sarcomere length, and l represents the distance between successive binding positions.

2.6 Limitations of Mechanical Models

While the Hill-based muscle models may be sufficient for various applications, their capacity is inherently limited in achieving highly accurate and realistic motion. First, they oversimplify muscle architecture, such as uniform fiber length, pennation angle, line of action and moment arm. Real muscles often have highly complicated structure and architectural variation (see Figure 2.6). This complexity may greatly influence the functional capacity of muscles.

Second, their unidirectional behavior cannot incorporate any lateral forces that may occur across the fibers. Neither for fiber to fiber

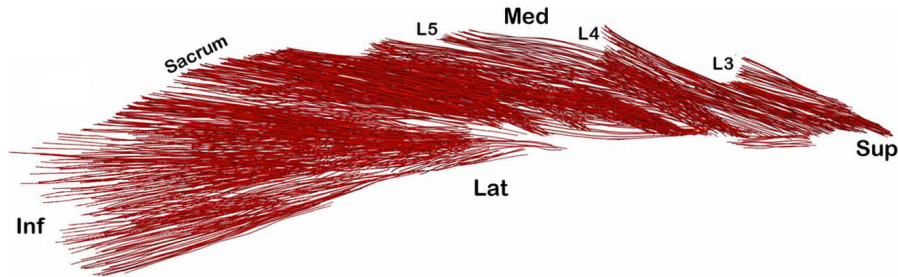


Fig. 2.6 Digitized *lumbar multifidus* ([67]).

interaction, nor also any passive motion induced by other tissue components, such as neighboring muscles or bones, can be easily accommodated. The interaction with other tissues may be important to represent *in vivo* muscle behaviors [13]. Constraint points or wrapping surfaces are commonly used to prevent the muscle from penetrating into other tissues. However, it is challenging to specify these constraints accurately. Third, their tendinous attachments to bones are modeled pointwise. This often makes it difficult to model complex muscles with broad tendinous attachments (e.g., *pectoralis major*). Last, the force production of skeletal muscle has hysteresis, namely history-dependent properties: force depression and force enhancement [30]. While force depression is produced by shortening of an activated muscle, force enhancement is caused by stretching or lengthening of an activated muscle. Thus, movement control and voluntary force production are affected by the contractile history of the muscle. The Hill-based and Huxley-based muscle models do not explicitly account for these properties.

3

Muscle Deformation

Muscle is not only a functional unit that drives body movement; it is also a fundamental component in defining the visual appearance of the human body. As such, realistic muscle deformation is needed for high-quality animated human characters. Several approaches have been proposed to model either muscle deformation or muscle-driven body deformation. Their application can be used to simulate different scales of systems, from a single muscle to an entire body. Based on their underlying fundamental methodology, we classify these approaches into three categories: geometrically-based, physically-based, and data-driven approaches.

3.1 Geometrically-Based Approaches

Geometrically-based techniques were employed in early systems because they are practical and efficient. Most proposed approaches have focused on modeling animation effects of muscle contraction, such as bulging or swelling, which can be the key underlying factors for skin deformation or facial animation. They have been shown to be successful

in modeling simple muscle (e.g., fusiform) but there may not be a straightforward extension to complex muscles [69, 89]. Furthermore, since muscle deformation is determined by skeleton arrangement, these techniques have difficulty in achieving a high order of realism from physiological or biomechanical perspectives. Thus, to better handle these problems, muscles are constructed as multiple layers or are often coupled with other physically-based approaches (see Section 3.2).

3.1.1 Space and Free Form Deformation

A space deformation is a mapping from an input domain to a target domain within an Euclidean space, in which geometric control is manipulated to satisfy specified constraints. The Free Form Deformation (FFD) technique places a lattice around an object and creates a deformable space by using a trivariate Bézier volume defined by the points of the lattice [70]:

$$X(u, v, w) = \sum_{i=0}^l \sum_{j=0}^m \sum_{k=0}^n B_i(u) B_j(v) B_k(w) P_{ijk}, \quad 0 \leq u, v, w \leq 1 \quad (3.1)$$

where $B_i(u)$, $B_j(v)$, and $B_k(w)$ are separable Bernstein polynomials and P_{ijk} is a point of the lattice (i.e., control point) and $X(u, v, w)$ is a deformed point (i.e., spatial point). Chadwick et al. [17] employed FFD to represent muscle deformation. Articulated skeletons, located inside muscle, transform a surrounding FFD lattice, which in turn represents a muscle shape change. Although FFDs provide simple and fast control, they do not permit direct manipulation of muscle shape. Also, the regular lattice spacing used by FFD prevents the detailed control needed to produce more refined and complex shapes (see Figure 3.1). Moccozet et al. [54] addressed this limitation by introducing Dirichlet Free From Deformation (DFFD) which is based on a scattered data interpolation technique. They removed the requirement for regularly spaced control points by replacing rectangular local coordinates by generalized natural neighbor coordinates (namely, Sibson coordinates). Given a point, its natural neighbors are collected based on Delaunay and Dirichlet/Voronoi diagrams and its displacement is computed using interpolation. They used a multi-layered deformation model to

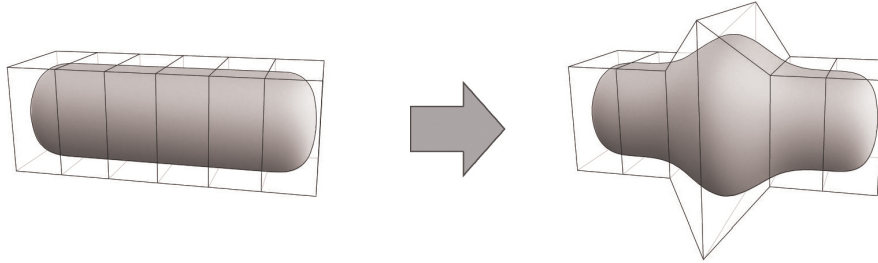


Fig. 3.1 An exemplary FFD surface is defined by a control lattice around the muscle shape surface. (*Left*) The FFD surface before deformation. (*Right*) The FFD surface after deformation.

illustrate hand animation in which the muscle layer is modeled by a DFFD control point set corresponding to a simplified hand topography. In Skeleton-Subspace Deformation (SSD), deformation of surface points is determined by the weighted summation of the associated skeleton coordinate transformations. Muscle bulging or swelling can be modeled by manually defining skeleton subspaces and adjusting weights. Lewis et al. [49] introduced the Pose-Space Deformation (PSD) by generalizing the interpolation domain, which can be defined by a skeleton or even expression parameters. They improved upon the blending problem, in which neighboring subspaces might incorrectly blend together in SSD, and permitted direct manipulation of the desired deformation.

3.1.2 Parametric and Polygonal Surfaces

A parametric surface is represented by either parametric equations to control shapes or a collection of surface patches which are defined in terms of bivariate and single valued equations (i.e., $x = x(u, w)$, $y = y(u, w)$, $z = z(u, w)$). A polygonal surface is an approximate and discretized surface represented by many simple geometric primitives, such as vertices, edges, and faces.

Komatsu [40] used biquartic Bézier surfaces to model body deformation. The Bézier surfaces are patched cylindrically around the skeleton and are jointly controlled to transform the body. Wilhelms [89] and Scheepers et al. [69] used a parametric ellipsoid as a basic primitive

to model human skeletal muscles. Three principal axes are adjusted to represent the bulging of the muscle belly, while volume is preserved with respect to constrained ratios using predefined relationships among these three axes. Although an ellipsoid is sufficient for modeling simple shapes, such as fusiform muscle, it cannot be easily adapted to model more complex muscle shapes. Scheepers et al. extended their model to represent multi-belly muscles (e.g., pectoralis) in which n pairs of origin and insertion points are specified and n ellipsoids are laterally aligned along the path within the corresponding pair. Their model is further generalized to represent more complex muscles which are bent and wrapped around anatomical structure (e.g., brachioradialis in the forearm). The straight path between the origin and the insertion point is replaced by a cubic Bézier curve representing the direction of muscle force and ellipses of varying size along this curve to define the volume and shape of the muscle. Dow and Semwal [23] proposed the generalized cylinder based muscle model, in which muscle is represented by a cylinder axis and surrounding cross-sectional slices. The contour of each slice is modeled by B-spline curves and its radius is controlled to express volumetric changes of muscle (see Figure 3.2). Wilhelms and Gelder [90] presented a similar approach with the additional flexibility that a cylinder axis can be bent for modeling muscle bent over a joint. Furthermore, the muscle length, width and, thickness are scaled to maintain constant volume. Ng-Thow-Hing and Fiume [58, 59] used B-spline solids in which a cylindrical coordinate system is chosen to construct a control point lattice from real specimen data. Their geometric parameterization can model realistic muscle shape and also depict muscle fibers inside the muscle.

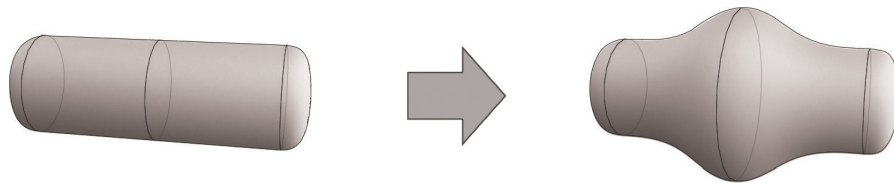


Fig. 3.2 An exemplary parametric and polygonal surface: a muscle shape is defined by control of a set of cross-sectional slices. The surface before deformation (*left*) and after deformation (*right*).

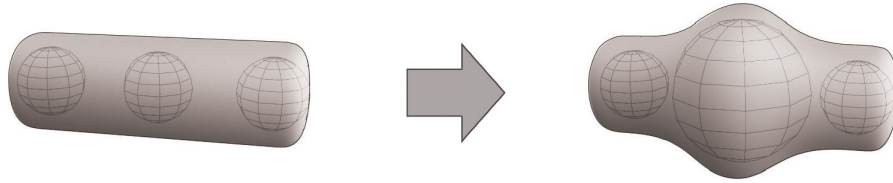


Fig. 3.3 An exemplary implicit surface is defined by the sum of field functions around associated spherical skeletons. The surface before deformation (*left*) and after deformation (*right*).

3.1.3 Implicit Surfaces

An implicit surface generated by a set of skeletons, s_i ($i = 1, 2, \dots, n$), with associated field functions, f_i , is defined at the isovalue c by

$$\{P \in \mathbb{R}^3 \mid f(P) = c\}, \quad \text{where } f(P) = \sum_{i=1}^n f_i(P). \quad (3.2)$$

The skeleton, s_i , can be any geometric primitive such as a point, a curve, a parametric surface, etc. The field function, f_i , is generally a decreasing function of the distance from a given point, P , to the associated skeleton (see Figure 3.3). Based on the type of field function, various implicit surfaces have been developed: blobs, metaballs, soft objects, and convolution surfaces [14, 15, 92].

Bloomenthal et al. [15] used convolution surfaces to model the human hand and arm by approximating bones, muscles, tendons and veins close to the underlying skeletons. Thalmann et al. [83] presented the multi-layered human model whose body primitives (e.g., muscle, limb, and fatty tissue) are additively constructed from a stick figure skeleton model and coated with the ellipsoidal metaball surfaces. Although the implicit surfaces are smooth and continuous in modeling objects, unwanted blending effects may often occur in modeling deformation over joints. This problem can be avoided by defining neighboring areas between the different skeletons, and specifying how the contributions from them are to be summed (e.g., blending graph [16] and weighted blending with the proximity [72]).

3.2 Physically-Based Approaches

While geometrically-based models have proven to be sufficient for some graphical applications demanding visually acceptable quality, their

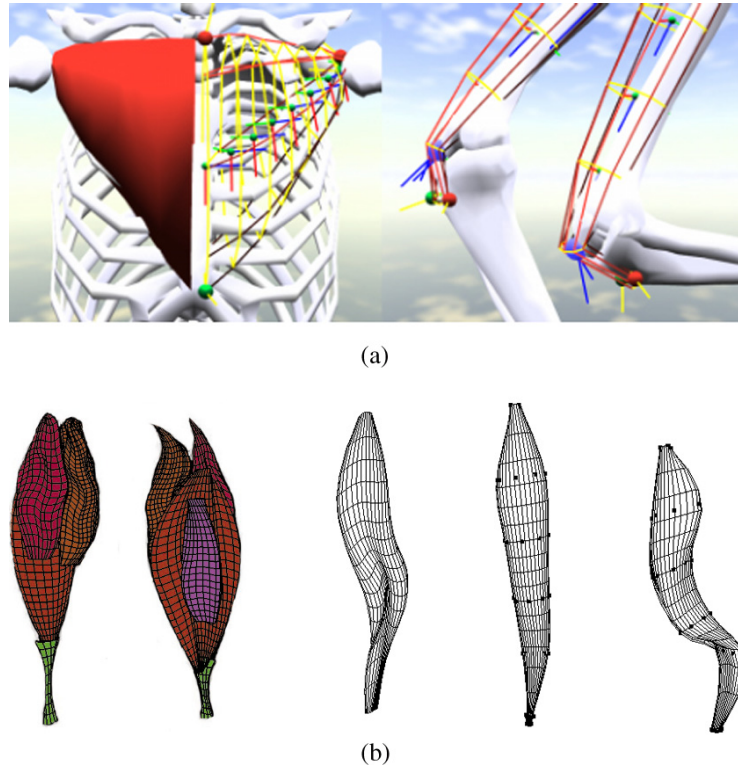


Fig. 3.4 Geometrically-Based Approaches. (a) deformed cylinders [89] and (b) B-Spline solids [58].

inherent simplicity and the need for human intervention often makes it difficult to extend them to represent complex scenes involving dynamics (Figure 3.4). Furthermore, they lack the physical or mechanical accuracy often required for realistic modeling and simulation. To overcome these deficiencies, many researchers have turned to physically-based approaches in which physical simulation is employed to solve for complex interactions involving muscle dynamics and tissue properties. To model physically-based muscles, the following two problems must be addressed: (1) determining the contractile muscle forces and (2) representing the changing muscle geometry during the contraction. To solve these problems, several muscle models have been proposed based on a variety of computational methods, such as mass-spring systems, FEM (Finite Element Method), and FVM (Finite Volume Method).

3.2.1 Mass-Spring System

An object is modeled by a collection of point masses linked together with massless springs. An elastic force acting on mass i connected by a spring to mass j is given by

$$\mathbf{f}_{ij} = k(|\mathbf{x}_{ij}| - l_{ij}) \frac{\mathbf{x}_{ij}}{|\mathbf{x}_{ij}|}, \quad (3.3)$$

where $\mathbf{x}_{ij} = \mathbf{x}_j - \mathbf{x}_i$, and $\mathbf{x}_i, \mathbf{x}_j$ are the locations of point masses i and j , respectively, l_{ij} is the rest length between them, and k is the spring's stiffness. This linear spring model can be generalized by incorporating various types of spring forces, such as angular, bending, and shearing. Each force is derived from an energy minimization principle and serves as a constraint to cause the desired deformation effects.

Chadwick et al. [17] linked FFD control points to point masses in a mass-spring system, allowing this dynamic system to influence the geometrically-based deformation. By augmenting their FFD-based muscle model with a mass-spring system they were able to represent the viscoelastic properties that articulated skeleton-driven deformation often lacks. Lee et al. [45] and Albrecht et al. [4] embedded a muscle layer based on a mass-spring system between the skin surface and the skeleton structure to model facial expressions and hands, respectively. Spring forces generated by the movement of bones in the skeleton caused the attached skin surface to deform realistically. Nedel and Thalmann [57] and Aubel and Thalmann [10] proposed a two-layered muscle model consisting of a line of action and the muscle surface. The line of action is modeled using either a straight line [57] or a 1D mass spring [10] to define the profile of the muscle (e.g., orientation and bone attachment). The skeleton kinematically controls the line of action to deform the surrounding muscle surface based on a mass spring system (see Figure 3.5(a)). Besides linear springs representing the surface, angular springs have been incorporated to control the volume of the muscle [57]. Ng-Thow-Hing and Fiume [58, 59] proposed a more sophisticated model based on anatomical and biomechanical considerations. Their solid muscle is extracted from medical imaging data or cross-sectional sliced images (e.g., Visible Human [2]) and modeled using volumetric B-splines. For interior details, a muscle

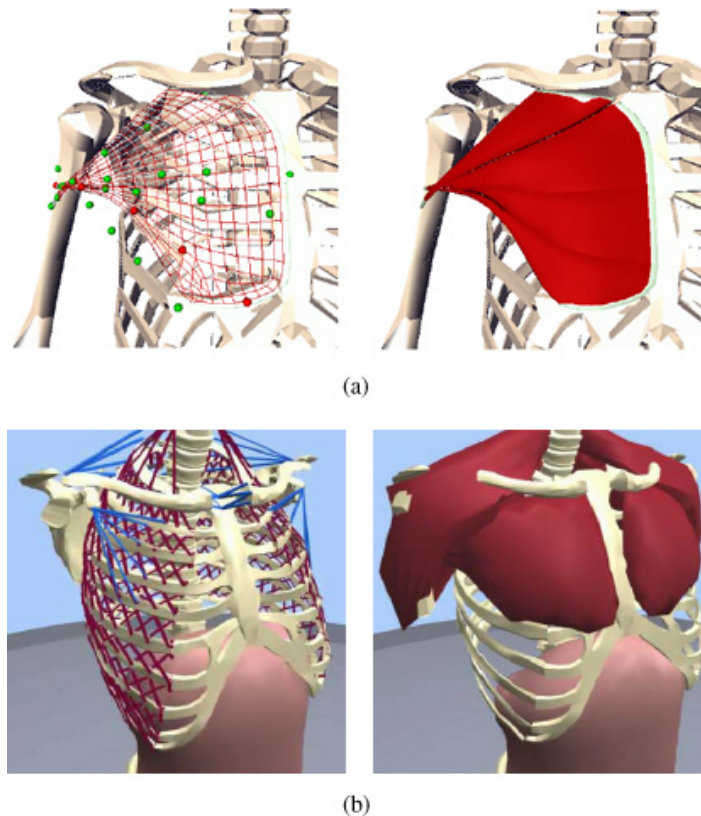


Fig. 3.5 A mass-spring system is used to simulate behaviors of lines of action and wrapped surfaces of (a) pectoralis muscle [10] and (b) torso model [98].

fiber architecture is constructed based on digitally scanned fiber data. While a Hill-based model is employed to express the dynamics of muscle fiber, a mass-spring system is used to represent viscoelastic deformation of muscle. Zordan et al. [98] developed a human torso model to animate breathing motions, such as inhalation and exhalation. The interplay of rib cage, diaphragm, and abdomen muscles while breathing was described based on respiration mechanics and was simulated using a mass-spring system (see Figure 3.5(b)). Furthermore, in order to preserve the volume of the human body, pressure forces based on anticipated volume change were incorporated. Delp et al. [21] used a set of line segments to define behavior of muscles. Additionally, wrapping

surfaces (e.g., ellipsoids and cylinders) are employed to impose geometrical constraints, preventing muscles from penetrating into other surrounding tissues.

3.2.2 Finite Element Method (FEM)

In the finite element method (FEM), a body is subdivided into a set of domains or finite elements (e.g., hexahedra or tetrahedra in 3D, quadrilaterals or triangles in 2D). Displacements and positions in an element are approximated from discrete nodal values using interpolation functions:

$$\Phi(\mathbf{x}) \approx \sum_i h_i(\mathbf{x})\Phi_i, \quad (3.4)$$

where h_i is a basis function and Φ_i is the scalar weight associated with h_i . There exist many choices for the element type and the basis functions. The choice depends on the object geometry, accuracy requirements, and computational budget. Higher order interpolation functions and more complex elements require greater computation per element, but may give a more accurate approximation. For a more complete discussion of the FEM, see [78]. Given a dynamic problem to be solved, equilibrium equations are derived in terms of quantities of interest (e.g., strain or stress) and are expressed as Partial Differential Equations (PDEs). These PDEs are then approximated by the FEM. For example, to represent solid deformation, the total strain energy as the potential energy is carefully designed to express desired material response and then equilibrium equations are derived according to the principle of *virtual work* [27, 56]. Resulting algebraic equations form a linear or nonlinear system, depending on the specified strain energy. While smaller linear systems can be solved by direct methods (e.g., Gaussian Elimination), large or nonlinear systems require iterative methods (e.g., Conjugate Gradient or Newton's method) [66].

Chen and Zeltzer [18] proposed a biomechanical approach by integrating a Hill-based muscle model into a linear elastic solid model. Active muscle forces are approximated as parametric functions and embedded into selected edges between vertices of a FEM-based

solid. While they animated flexion of muscles, they emphasized the biomechanical validity of their model by comparing it to experimental measurements, such as the force-length and quick-release properties. Zhu et al. [97] employed Stern's muscle model [77] in which simplified behaviors of bone-joint-muscle complexes are described. Both works employed a linear elastic material model for connective passive tissues of muscle, which is computationally efficient but valid only for infinitesimal deformation. In contrast, Hirota et al. [32] and Lemos et al. [46] adopted nonlinear material models that allowed the robust representation of large deformations. Hirota et al. combined the Mooney-Rivlin model [55], the Veronda model [88] and the fiber-reinforcement material model [39] to express passive response of tissues during body contact. Lemos et al. [46] used a rubber-like material model (e.g., hyperelastic material) and explicitly aligned Hill-based muscle forces to fiber orientations within the finite elements.

In biomechanics, FEM has been widely investigated for studying skeletal muscles. Various muscle models have been proposed to analyze and predict accurate strain distribution of muscle during contraction and its functional properties. Yucesoy et al. [93] modeled the mechanical behavior of skeletal muscle as the interaction between the intracellular domain (i.e., muscle fibers) and extracellular matrix domain (i.e., connective tissues). Thus, muscle geometry is represented by two separate meshes that are elastically linked to account for the force transmissions between these two domains. Blemker and Delp [13] and Blemker [12] developed a way to represent complex muscle geometry and architecture (see Figure 3.6(a)). A variation of the moment arms of fibers is modeled and the predicted changes to muscle shape are compared to magnetic resonance images. Tang et al. [80] proposed a constitutive muscle model in which active contraction of muscle fibers and hyperelastic material properties are coupled using the strain energy approach. They demonstrated different types of contractions, such as concentric and eccentric contractions, and effects of muscle geometry and fiber orientation on the stress distribution. The work by [28, 61] incorporated the Huxley model to represent contractile properties of skeletal muscle. The Huxley equations (Equation 2.3) are approximated using a Distribution Moments

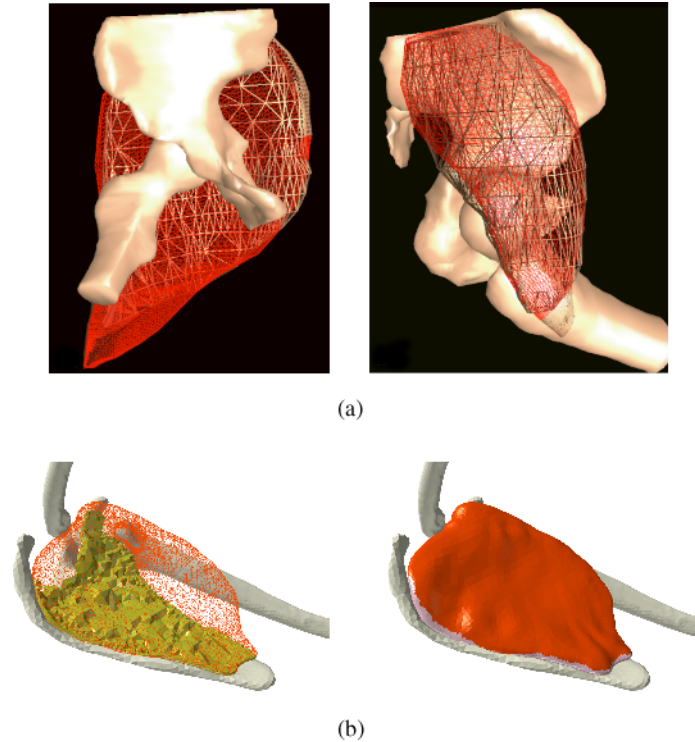


Fig. 3.6 Physically-based Approaches: (a) gluteus maximus and medius muscle models with the hip extension and flexion (based on FEM, [12]) and (b) subscapularis muscle model attached to scapula bone model (based on FVM, [82]).

approach [94] and combined with the constitutive equation describing nonlinear and incompressible material response.

3.2.3 Finite Volume Method (FVM)

As with FEM, the finite volume method approximates PDEs piecewise by algebraic equations. More specifically, for the integration of conserved variables in PDEs, volume integrals are converted to surface integrals using the divergence theorem. These terms are then evaluated as fluxes at the surfaces of each finite volume. For example, to compute the internal force \mathbf{f} at node \mathbf{x}_i , we use

$$\mathbf{f}_i = \frac{d}{dt} \iiint_{\Omega_i} \rho \mathbf{v} d\mathbf{x} = \frac{d}{dt} \iint_{\partial\Omega_i} \mathbf{t} dS = \frac{d}{dt} \iint_{\partial\Omega_i} \boldsymbol{\sigma} \mathbf{n} dS, \quad (3.5)$$

where Ω_i is a small volume containing \mathbf{x}_i , ρ is the density, \mathbf{v} is the velocity, \mathbf{t} is the surface traction on $\partial\Omega_i$, σ is the stress tensor, and \mathbf{n} is the surface normal. As we read from left to right in (3.5), note that computationally the volumetric integral requiring velocities and densities to be defined at every point in space are replaced by the computation of a potentially more tractable stress tensor and normal on a surface boundary. For a more complete discussion of the FVM, see [47].

Teran et al. [81, 82] proposed a FVM-based approach to simulate deformable behavior of skeletal muscles (shown in Figure 3.6(b)). They argued that FVM inherently requires less computation and memory usage than FEM does. Moreover, they showed that FVM provides a geometric interpretation of stress inside the object (i.e., multidimensional forces pushing on each face of an element), allowing for a simpler and more intuitive way of integrating equations of motion compared to FEM. To represent highly nonlinear material response of muscle, they used a sophisticated constitutive model similar to [32]. Furthermore, they incorporated anisotropic properties based on fiber architecture, which are modeled using the B-spline solid technique [59].

3.3 Data-Driven Approaches

In contrast to many methods involving the modeling of physical human components and processes, some data-driven approaches forego anatomical mechanisms and directly model the skin shape in an “outside-in” manner, deformed by the underlying muscle, of a human in plausible poses. Data is captured on the surface of subjects usually with markers on the skin by a motion capture system or a range scanning device. Several techniques may then be used to generate a new skin surface given a novel skeleton pose. Although such data-driven approaches are relatively new, several key papers have already shown the power of this technique.

Early work by Min et al. [53] is based on the observation that skin shape in a human scan is determined by the underlying skeleton and muscle, and uses an anatomically-based approach having layers of skeleton, muscle, and skin. Moving the skeleton deforms the isosurface

muscle in a volume-preserving fashion, which in turn deforms the skin layer. The upper body was modeled and the resulting animation showed realistic arm bending and stretching. Another approach to arm animation by Sloan et al. used several exemplary arm shapes [73] and a unique interpolation scheme using linear and radial basis functions to create a continuous range of well-behaved poses.

As example poses of human subjects became more accessible, more ambitious systems were created [51]. In the range-scanning technique, a person poses for a short time as a scanner creates tens of thousands of data points on the surface of the subject at a density of just a few millimeters. Allen et al. [5] created a high quality posable upper body model from range scan data together with many correspondence markers. This work was later expanded [6], to accommodate the large CAESER (Civilian American and European Surface Anthropometry Resource project) database of whole-body range scans, resulting in a compelling system with several desirable features. Morphing by interpolating between registered scans or fitting a model to a sparse marker set are two significant outcomes of this technique (see Figure 3.7). The technique also supports transferring texture, surface data or animation between models to correct scanning problems, to alter the appearance, or to animate the characters. Multiple correlated parameters could be modified, such as a person's weight or height, or statistically correct human shapes could be preserved when locally modifying a character part, for example, lengthening an arm.

There are many steps involved in creating the reconstruction and parameterization of the CAESER data sets. Previous techniques, which were used primarily on morphable face models, were based on

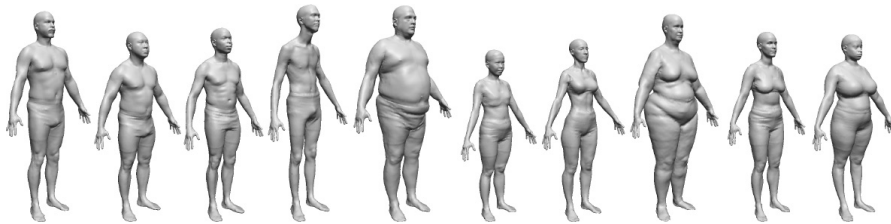


Fig. 3.7 Data-driven approach: statistical model [6].

cylindrical mappings that could not be adapted to a complex branching object, like the complete human body. This review used an artist-generated template object together with a nonrigid registration technique to create a vertex correspondence between a set of skin surfaces that have substantial variation in shape, but a common overall human structure. An energy-minimization approach was used with a weighted sum error objective function that combines distance to a template object, smoothness, and marker distance.

Seo and Thalmann [71] presented a similar template-based system with additional tailoring parameters to generate new, instantly animatable, high-quality human forms, ideal for fashion design. An alternate technique uses many silhouettes from a video stream instead of range scan data to formulate the human shape in a re-animatable form [68]. Anguelov et al. [9] extended this work, focusing on representing muscle deformation resulting from articulated body motion, to perform Shape Completion and Animation of People (SCAPE), by using separate models for pose deformation and for body shape variation. By decoupling the skeleton (rigid) deformation from the muscle (nonrigid) deformation, the formulation, identification of the model, and the efficiency of the learning algorithms are all improved. A limitation is that a single muscle deformation model is used for all people so that a more muscular person may not exhibit as much muscle deformation as they should.

Data-driven modeling of skin and muscle deformation was further refined by Park and Hodgins [64, 65] by modeling static deformations, as a function of skeleton pose, and dynamic deformations, as

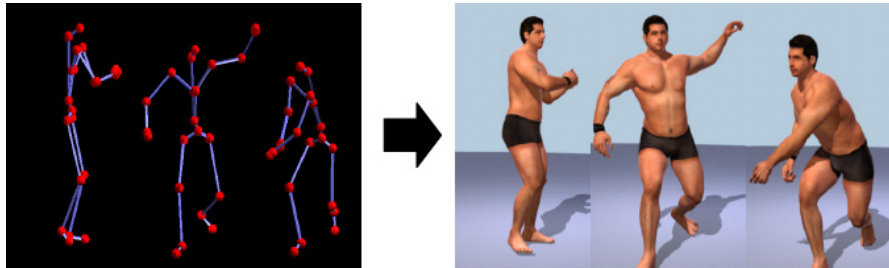


Fig. 3.8 Data-driven approach: motion-capture [65].

a function of the acceleration of each body part. Animated motions of an actor were captured using a high density of 350 markers, while performing slow motions and then fast motions. The two classes of deformation were then modeled and new animations could be generated from more typical marker counts (40 to 50 markers) in additional motion-capture sessions. Although this approach still has the limitation of being skeleton-driven and does not express muscle motion without joint angle changes, it does produce very high quality results (see Figure 3.8).

4

Control and Simulation

While Section 3 examined various approaches proposed to represent deformable behavior of skeletal muscles, this section reviews numerous simulation models which were developed to control muscle functions, producing realistic human movement. In general, the musculoskeletal system is modeled as a combination of three sub-models: activation dynamics, contraction dynamics, and skeleton dynamics. Activation dynamics describe dynamic relations between the neural excitation and muscle activation, which is often modeled using first order Ordinary Differential Equations (ODEs) as

$$\frac{da_j}{dt} = (u_j - a_j) \left(\frac{u_j}{\tau_{\text{act},j}} + \frac{1 - u_j}{\tau_{\text{deact},j}} \right), \quad (4.1)$$

where u_j , a_j , $\tau_{\text{act},j}$, and $\tau_{\text{deact},j}$ are the neural excitation, muscle activation, activation time constant and deactivation time constants of muscle j , respectively. Contraction dynamics relates muscle activation to the resulting muscle forces by taking into account physiological features of muscle, such as fiber arrangement and passive tissue properties. A Hill model is commonly used to model contraction dynamics (see Section 2.5). Skeleton dynamics accounts for the relationship between

muscle forces, external constraints, and resulting skeletal motions:

$$M(\mathbf{q})\ddot{\mathbf{q}} + c(\mathbf{q}, \dot{\mathbf{q}}) + g(\mathbf{q}) - S(\mathbf{q})\mathbf{f}_{ext} = R(\mathbf{q})\mathbf{f}_{mt}, \quad (4.2)$$

where \mathbf{q} , $\dot{\mathbf{q}}$, $\ddot{\mathbf{q}}$ are vectors of the generalized coordinates of joints, velocity, and acceleration, respectively. $M(\mathbf{q})$ is the generalized inertia matrix, $c(\mathbf{q}, \dot{\mathbf{q}})$ is the vector of generalized Coriolis and centrifugal forces and $g(\mathbf{q})$ is the vector of the generalized gravitational forces. $S(\mathbf{q})$ and $R(\mathbf{q})$ denote the geometric transformation matrices of the generalized external forces (\mathbf{f}_{ext}) and musculotendon forces (\mathbf{f}_{mt}) to the joint forces, respectively. To obtain $M(\mathbf{q})$, the mass of the muscle is lumped along with associated skeletal and soft tissues within a body segment. Although this method is widely used in practice, a significant error can be induced in the associated simulation model because (4.2) does not model the movement of the mass of the muscle in the direction of stretching and shortening during movement [62]. Upon generating skeletal motions using (4.2), driving muscle forces can be computed using either manually-specified profiles (e.g., handcrafted curves [18], sinusoid [85, 98], and key-framed control [81]) or computationally-predicted values of muscle activation (e.g., [44, 79, 84]). In biomechanics, the computation of muscle functions has been systematically studied through rigorous experiments, and a variety of simulation models has been developed and validated against experimental data. As the complexity of desired motion increases or more realistic representations are required in human animation, the usage of these simulation models becomes more advantageous due to their reliability, consistency, and accuracy.

However, determination of muscle functions is challenging due to the high redundancy of the human musculoskeletal system: the number of contributing muscles is greater than the number of degrees of freedom specifying skeletal motion, leading to an underdetermined problem. This difficulty is often handled by using optimization approaches, which are generally classified into static and dynamic optimization. They are generally formulated as finite, constrained problems, or nonlinear optimization problems of the control parameters. These optimization problems are commonly solved by sequential quadratic programming

methods [60]. We briefly describe below the static and dynamic optimization approaches and review simulation models based on them.

4.1 Static Optimization

Static optimization (also referred to as inverse dynamics) takes non-invasive measurements of body motions, such as position, velocity, acceleration, and external loads, as inputs to (4.2) to calculate muscle forces (see Figure 4.1). An instantaneous motion of the skeleton at each time instant is translated into algebraic equations that specify desired criteria through a set of constraints (e.g., $0 \leq F_{mt} \leq F_{mt}^{\max}$) or objective functions. A typical objective function is the minimization of total muscle force or activation amplitude [19]:

$$J = \sum_{i=1}^n \left(\frac{F_{mt,i}}{\text{PCSA}_i} \right)^2 \quad (4.3)$$

where $F_{mt,i}$ is the force applied by muscle i at time instant t , PCSA_i is the physiological cross-sectional area of muscle i , and n is the number of muscles. In static optimization, because there is no dynamic dependence between muscle forces at different time instants, time integration is not necessary, which makes the problem computationally simpler. However, it is difficult to integrate muscle physiology (e.g., excitation and activation dynamics) and the objective of the motor tasks

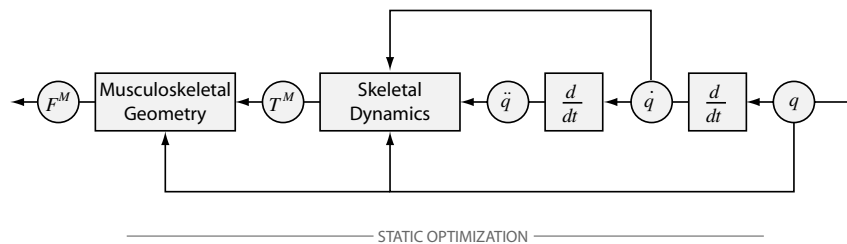


Fig. 4.1 Static optimization (or inverse dynamics) pipeline. Body motions are prescribed as inputs and optimal muscle forces are determined as outputs. (Adapted from [96]).

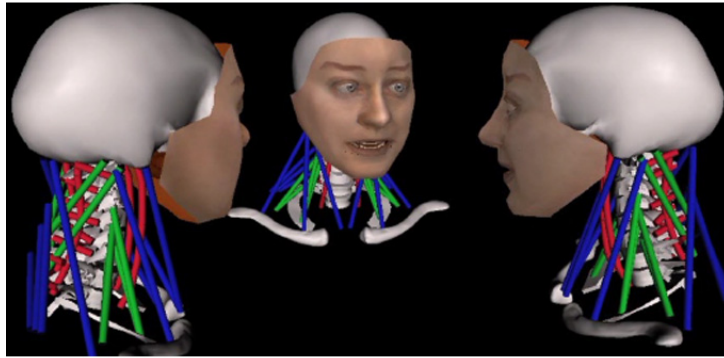
(e.g., maximum height jumping). Furthermore, the validity of this approach is highly dependent on the accuracy of the experimental measurement of motions.

Komura et al. [42, 41] computed muscle activation from key-framed postures of human lower extremities while minimizing total torque changes and activation amplitude. Their model was further extended to consider some physiological features, such as muscle fatigue and injury [41]. Tsang et al. [84] presented a musculotendon model of the human hand and forearm. Their model features both inverse and forward simulation. Given motion capture data or key-framed animation, an optimal set of muscle activations is determined using the static optimization method and then taken as input to a forward simulation of the model to achieve the desired pose or motion. Their optimization criteria are formulated based on the minimization of the kinematic error between computed and measured motion, and the total amount of muscle contraction.

Lee and Terzopoulos [44] proposed a hierarchical approach to simulate the head and neck system (see Figure 4.2(b)), which is controlled by a higher-level voluntary sub-controller and a lower-level reflex sub-controller. The voluntary controller generates feedforward neural signals with respect to the desired pose, muscle tone (i.e., stiffness), and feedback gains based on monitored current motion. Upon their receipt, the reflex controller determines activation and co-activation of muscles, and modulates strain and strain rate of muscles in response to their current state. An artificial neural network is employed to model these voluntary controllers and they are trained offline to precompute feedforward signal functions of the target pose. This approach was extended to simulate a complete human upper body by integrating trunk and arm models [43]. As well as the muscle-based skeletal dynamics, a physics-based soft tissue simulator was incorporated to represent realistic flesh deformation during body movement. Kim et al. [38] optimized several motion tasks based on the hypothesis that total energy consumption governs human motion. The energy is described as the heat generated by muscle and formulated in joint space. Optimal joint kinematic profiles are computed while minimizing total energy expended at each time interval. Various tasks with different goals were simulated and



(a)



(b)

Fig. 4.2 Static optimization: (a) musculotendon simulation for hand ([79]) and (b) neuro-muscular simulation for head and neck ([44]).

demonstrated in the virtual human environment, *Santos* [1]. Sueda et al. [79] presented a musculotendon simulation of a human hand, in which behaviors of muscles and tendons are governed by spline-based strand dynamics (see Figure 4.2(a)). The strand dynamics are formulated by coupling muscle contraction and constraint forces based on routing of muscle and tendons. The optimal muscle activation is computed with respect to minimized total activation and proper damping. Fels et al. [24] and Stavness et al. [74, 75] proposed dental applications to model and simulate the oral, pharyngeal and laryngeal complex based on the *ArtiSynth* platform [50], in which associated muscle activation is predicted for jaw-tongue movement and hyolaryngeal elevation during chewing and swallowing. As a generalized simulation framework, Damsgaard et al. [20] developed the *AnyBody Modeling System* which is capable of modeling and analyzing full body complexity for various motions.

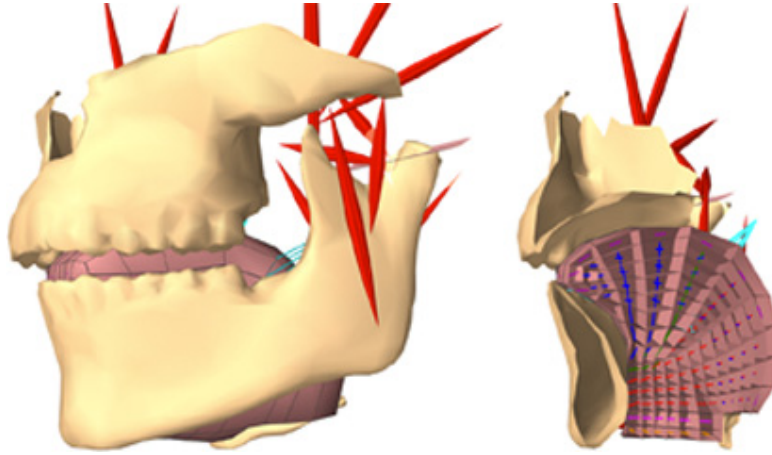


Fig. 4.3 Static optimization: simulation for the jaw-tongue-hyoid dynamics ([76]).

4.2 Dynamic Optimization

Dynamic optimization (also referred to as forward dynamics) is generally formulated by combining (2.2), (4.1), and (4.2), taking muscle excitation as inputs to produce body motion and then determining the optimal excitation trajectory while satisfying performance criteria (see Figure 4.4). While static optimization only accounts for each time instant, dynamic optimization considers the entire duration of movement, requiring the time integration of (4.2). Dynamic optimization is much more computationally expensive than static optimization. However, in contrast to static optimization, physiological, and time-dependent properties can be incorporated. Also, desired motor tasks can be formulated as performance criteria, such as minimum-time kicking [29], maximum-height jumping [63], and maximum-distance throwing [33]. Anderson and Pandy [7, 8] employed the minimization of metabolic energy expenditure [86] per unit distance which is assumed to characterize human gait during normal walking. Anderson and Pandy [8] showed that static optimization and dynamic optimization lead to similar results in predicting muscle forces and joint contact forces during normal human walking. They argued that this similarity is due to the fact that minimizing muscle fatigue at each time instant

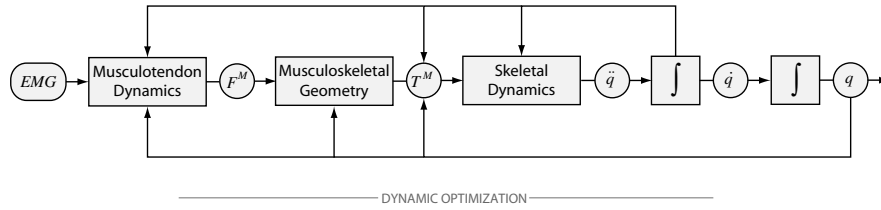


Fig. 4.4 Dynamic optimization (or forward dynamics) pipeline: muscle excitation is prescribed as inputs and the resulting skeletal motion is used to determine optimal excitation. (Adapted from [96]).

is roughly the same as minimizing metabolic energy expended per unit distance traveled over the complete gait cycle. Also, they pointed out that physiological properties, such as the force-length-velocity properties of muscle and activation dynamics, had little influence on static optimization.

5

Discussion and Conclusion

We have reviewed a variety of approaches for modeling muscle deformation and simulation of muscle functions. For modeling muscle deformation, geometrically-based approaches prevailed in early work because of their simplicity and efficiency. Although these techniques produce results that have limited accuracy and realism, they may still be appropriate solutions for some real-time applications, in that they provide intuitive and easy controls for designers to produce animations. On the other hand, physically-based approaches augmented with biomechanical and physiological considerations provide a high degree of visual quality and accuracy in modeling muscles. Despite high computational demands, their feasibility in applications continues to expand thanks in part to increasing computing power. Data-driven muscle and skin deformation modeling has advanced significantly in recent years. Only a few components in addition to those proposed by Park and Hodgins [65] are still needed to produce a complete system for computer graphics applications. Isometric muscle effects without joint-angle changes is still an outstanding problem as is the ability to drive existing models from new actors, which was available in other previous works. We are optimistic that, for the purposes of computer animation, a complete system will in future be created that is entirely data-driven.

For simulation of muscles, we have reviewed static and dynamic optimization, which can be viewed as complementary approaches. If external forces and body motions can be accurately measured, static optimization is preferred because it provides a practical and computationally efficient solution for estimating muscle forces. On the other hand, dynamic optimization offers a more reliable and stable solution. Also, if time-dependent performance criteria must be considered (e.g., maximum-height jumping) or if the aim is to investigate the influence of musculoskeletal structures on the function and performance of a motor task, dynamic optimization is required.

While significant progress has been made to date, there are still many issues for future work. We offer some suggestions which could be helpful for enhancing visual realism and accuracy in modeling muscle and ultimately the complete human.

First, many researchers have focused primarily on modeling muscles with simple internal architecture (e.g., parallel and fusiform) rather than complex pennate muscles. Moreover, current muscle models are often oversimplified by neglecting nonuniformity and irregularity that is clearly present in the architecture of real muscle specimens. The reason for this may be due to the limited availability of data and unknown physiological properties. However, to enhance anatomical and physiological accuracy, this complexity must be considered. Some invasive assessment techniques, such as those proposed by Agur et al. [3], Fung et al. [25] and Wu et al. [91], or non-invasive methods, such as diffusion tensor MRI [48], could be incorporated (see Figure 5.1). In addition to accurate reconstruction of muscle morphology, the effect of complex muscle structure on muscle deformation and physiological functions needs to be studied further. Validation against experimental measurements should be attempted.

Second, there is a need to solve contact problems that occur in muscle groups or between muscles and the underlying skeleton. This problem has been largely overlooked in previous approaches, which have presented models for the simulation of a single muscle in isolation or simple muscle-skeleton dynamics. Some researchers (e.g., [43, 44]) have used multiple muscles to coordinate body movements, but they did not address the issues associated with collision or contact between muscles.

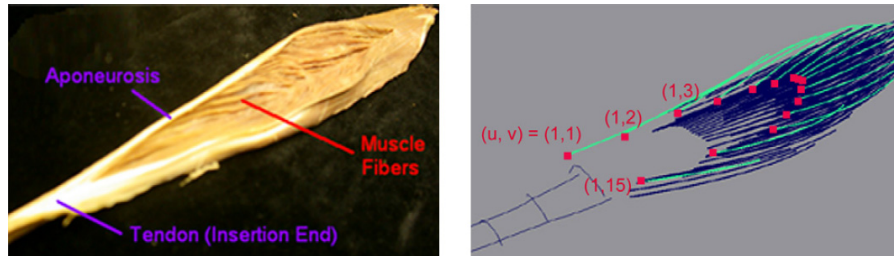


Fig. 5.1 Digitization and reconstruction of *extensor carpi radialis brevis* muscle ([91]).

This is a crucial omission, since most of our muscle systems, such as biceps, triceps, and quadriceps, are grouped together and intertwined. Furthermore, for realistic modeling and accurate simulation of body movement, a solution to the contact problem within muscle groups would produce a significant advancement in this area.

Third, biomechanical techniques could enhance visual realism and accuracy of controls in human animation. In biomechanics, significant progress has been made in understanding human movements through rigorous data capture and analysis. Recently, some simulation models have been introduced to provide more accurate, realistic, and automated controls for muscle-based animations [41, 43, 44, 84]. They have shown that the inclusion of biomechanical approaches can produce more accurate and realistic human models. This review is promising for various applications, such as ergonomics and medicine. However, biomechanical models are often too computationally expensive for use in graphics applications. Some informed simplification or approximation may be needed to obtain the efficiency needed for graphics applications.

Last, some physiological considerations could provide additional expressive controls in human modeling. For example, animation of human walking could be varied by specifying physiological or pathological effects, such as fatigue, which is related to the intra-muscular calcium level. Also, restriction of the activation range of certain muscles or muscle fibers could be used to model muscle related injury or disease. Although they can be manually controlled [84], simulation against external loads could yield promising results, which could be useful

not only for video games, but also for ergonomics and rehabilitation applications.

Ultimately, a unified model, scalable from visually realistic interactive systems to highly accurate offline patient-specific diagnostics systems, is the holy grail of this research area. While much still needs to be learned about detailed muscle architecture, human variation, and human muscle coordination strategies, progress is being made both in computer graphics and biomechanics. We believe that more extensive collaboration between these research communities will result in significant advancements toward a unified model.

Acknowledgments

This research was supported in part by the Natural Sciences and Engineering Research Council (NSERC) of Canada.

References

- [1] K. Abdel-Malek, J. Yang, J. H. Kim, T. Marler, S. Beck, C. Swan, L. Frey-Law, A. Mathai, C. Murphy, S. Rahmatallah, and J. Arora, "Development of the virtual-human Santo," in *Proceedings of the International Conference on Digital Human Modeling*, pp. 490–499, 2007.
- [2] M. Ackerman, "The Visible Human Project," in *Proceedings of IEEE*, vol. 86, pp. 504–511, 1998.
- [3] A. M. Agur, V. Ng-Thow-Hing, K. A. Ball, E. Fiume, and N. H. McKee, "Documentation and three-dimensional modelling of human soleus muscle architecture," *Clinical Anatomy*, vol. 16, no. 4, pp. 285–293, 2003.
- [4] I. Albrecht, J. Haber, and H.-P. Seidel, "Construction and animation of anatomically based human hand models," in *SCA '03: Proceedings of the 2003 ACM SIGGRAPH/Eurographics Symposium on Computer Animation*, pp. 98–109, Aire-la-Ville, Switzerland, Switzerland: Eurographics Association, 2003.
- [5] B. Allen, B. Curless, and Z. Popović, "Articulated body deformation from range scan data," *ACM Transactions on Graphics*, vol. 21, no. 3, pp. 612–619, 2002.
- [6] B. Allen, B. Curless, and Z. Popović, "The space of human body shapes: reconstruction and parameterization from range scans," in *SIGGRAPH '03: ACM SIGGRAPH 2003 Papers*, pp. 587–594, New York, NY, USA: ACM, 2003.
- [7] F. C. Anderson and M. G. Pandy, "Dynamic optimization of human walking," *Journal of Biomechanical Engineering*, vol. 123, no. 5, pp. 381–390, 2001.
- [8] F. C. Anderson and M. G. Pandy, "Static and dynamic optimization solutions for gait are practically equivalent," *Journal of Biomechanics*, vol. 34, no. 2, pp. 153–161, 2001.

- [9] D. Anguelov, P. Srinivasan, D. Koller, S. Thrun, J. Rodgers, and J. Davis, "SCAPE: shape completion and animation of people," *ACM Transactions on Graphics*, vol. 24, no. 3, pp. 408–416, 2005.
- [10] A. Aubel and D. Thalmann, "Interactive modeling of the human musculature," in *Proceedings of Computer Animation*, pp. 125–135, 2001.
- [11] N. I. Badler and S. W. Smoliar, "Digital Representations of Human Movement," *ACM Computings Surveys*, vol. 11, no. 1, pp. 19–38, 1979.
- [12] S. Blemker, "3D modeling of complex muscle architecture and geometry," PhD Thesis, Stanford University, July 2004.
- [13] S. S. Blemker and S. L. Delp, "Three-dimensional representation of complex muscle architectures and geometries," *Annals of Biomedical Engineering*, vol. 33, no. 5, pp. 661–673, 2005.
- [14] J. F. Blinn, "A generalization of algebraic surface drawing," *ACM Transactions on Graphics*, vol. 1, no. 3, pp. 235–256, 1982.
- [15] J. Bloomenthal and K. Shoemake, "Convolution surfaces," in *SIGGRAPH Computer Graphics*, pp. 251–256, 1991.
- [16] M.-P. Cani-Gascuel and M. Desbrun, "Animation of deformable models using implicit surfaces," *IEEE Transactions on Visualization and Computer Graphics*, vol. 3, no. 1, pp. 39–50, 1997.
- [17] J. E. Chadwick, D. R. Haumann, and R. E. Parent, "Layered construction for deformable animated characters," in *SIGGRAPH Computer Graphics*, pp. 243–252, 1989.
- [18] D. T. Chen and D. Zeltzer, "Pump it up: Computer animation of a biomechanically based model of muscle using the finite element method," in *SIGGRAPH Computer Graphics*, pp. 89–98, 1992.
- [19] R. Crowninshield and R. Brand, "A physiologically based criterion of muscle force prediction in locomotion," *Journal of Biomechanics*, vol. 14, no. 11, pp. 793–801, 1981.
- [20] M. Damsgaard, J. Rasmussen, S. T. Christensen, E. Surma, and M. de Zee, "Analysis of musculoskeletal systems in the anybody modeling system," in *Simulation Modelling Practice and Theory*, pp. 1100–1111, 2006.
- [21] S. L. Delp and J. P. Loan, "A computational framework for simulating and analyzing human and animal movement," *Computing in Science and Engineering*, vol. 2, pp. 46–55, September 2000.
- [22] S. L. Delp, J. P. Loan, M. G. Hoy, F. E. Zajac, E. L. Topp, and J. M. Rosen, "An interactive graphics-based model of the lower extremity to study orthopaedic surgical procedures," *IEEE Transactions on Biomedical Engineering*, vol. 37, pp. 757–767, 1990.
- [23] E. Dow and S. Semwal, "A framework for modeling the human muscle and bone shapes," in *Proceedings of the Third International Conference on CAD and Computer Graphics*, pp. 110–113, 1993.
- [24] S. Fels, I. Stavness, A. G. Hannam, J. E. Lloyd, P. Anderson, C. Batty, H. Chen, C. Combe, T. Pang, T. Mandal, B. Teixeira, S. Green, R. Bridson, A. Lowe, F. Almeida, J. Fleetham, and R. Abugharbieh, "Advanced tools for biomechanical modeling of the oral, pharyngeal, and laryngeal complex," in *International Symposium on Biomechanics Healthcare and Information Science*, February 2009.

- [25] L. Fung, B. Wong, K. Ravichandiran, A. Agur, T. Rindlisbacher, and A. Elmaraghy, "Three-dimensional study of pectoralis major muscle and tendon architecture," *Clinical Anatomy*, vol. 22, no. 4, pp. 500–508, 2009.
- [26] H. S. Gasser and A. V. Hill, "The dynamics of muscular contraction," in *Royal Society of London Proceedings*, pp. 398–437, 1924.
- [27] S. F. F. Gibson and B. Mirtich, "A survey of deformable modeling in computer graphics," Technical Report, Mitsubishi Electric Research Laboratories, 1997.
- [28] A. W. J. Gielen, C. W. J. Oomens, P. H. M. Bovendeerd, T. Arts, and J. D. Janssen, "A finite element approach for skeletal muscle using a distributed moment model of contraction," *Computer Methods in Biomechanics and Biomedical Engineering*, vol. 3, no. 3, pp. 231–244, 2000.
- [29] H. Hatze, "The complete optimization of a human motion," *Mathematical Biosciences*, vol. 28, no. 1–2, pp. 99–135, 1976.
- [30] W. Herzog, "History dependence of skeletal muscle force production: Implications for movement control," *Human Movement Science*, vol. 23, no. 5, pp. 591–604, 2004.
- [31] A. Hill, *First and Last Experiments in Muscle Mechanics*. Cambridge at the University Press, 1970.
- [32] G. Hirota, S. Fisher, A. State, C. Lee, and H. Fuchs, "An implicit finite element method for elastic solids in contact," in *Computer Animation*, 2001.
- [33] M. Hubbard and L. Alaways, "Rapid and accurate estimation of release conditions in the javelin throw," *Journal of Biomechanics*, vol. 22, no. 6–7, pp. 583–595, 1989.
- [34] A. F. Huxley, "Muscle structure and theories of contraction," *Progress in Biophysics and Biophysical Chemistry*, vol. 7, pp. 255–318, 1957.
- [35] A. F. Huxley and R. M. Simmons, "Proposed mechanism of force generation in striated muscle," *Nature*, vol. 233, pp. 533–538, 1971.
- [36] R. H. Jensen and D. T. Davy, "An investigation of muscle lines of action about the hip: A centroid line approach vs the straight line approach," *Journal of Biomechanics*, vol. 8, no. 2, pp. 105–110, 2004.
- [37] D. Jones, A. D. Haan, and J. Round, *Skeletal Muscle — Form and Function*. Churchill Livingstone, 2004.
- [38] J. H. Kim, K. Abdel-Malek, J. Yang, and R. T. Marler, "Prediction and analysis of human motion dynamics performing various tasks," *International Journal of Human Factors Modelling and Simulation*, vol. 1, no. 1, pp. 69–94, 2006.
- [39] S. M. Klischab and J. C. Lotza, "Application of a fiber-reinforced continuum theory to multiple deformations of the annulus fibrosus," *Journal of Biomechanics*, vol. 32, no. 10, pp. 1027–1036, 1999.
- [40] K. Komatsu, "Human skin model capable of natural shape variation," *The Visual Computer*, vol. 3, no. 5, pp. 265–271, 1988.
- [41] T. Komura, Y. Shinagawa, and T. Kunii, "Creating and retargetting motion by the musculoskeletal human body model," *The Visual Computer*, vol. 16, no. 5, pp. 254–270, 2000.
- [42] T. Komura, Y. Shinagawa, and T. L. Kunii, "A muscle-based feed-forward controller of the human body," *Computer Graphics Forum*, vol. 16, no. 3, pp. C165–C176, 1997.

- [43] S.-H. Lee, E. Sifakis, and D. Terzopoulos, “Comprehensive biomechanical modeling and simulation of the upper body,” *ACM Transactions on Graphics*, vol. 28, no. 4, pp. 1–17, 2009.
- [44] S.-H. Lee and D. Terzopoulos, “Heads up!: Biomechanical modeling and neuromuscular control of the neck,” in *SIGGRAPH Computer Graphics*, pp. 1188–1198, 2006.
- [45] Y. Lee, D. Terzopoulos, and K. Walters, “Realistic modeling for facial animation,” in *SIGGRAPH Computer Graphics*, pp. 55–62, 1995.
- [46] R. Lemos, M. Epstein, W. Herzog, and B. Wyvill, “Realistic skeletal muscle deformation using finite element analysis,” in *Proceedings of the XIV Brazilian Symposium on Computer Graphics and Image Processing*, pp. 192–199, 2001.
- [47] R. J. LeVeque, *Finite Volume Methods for Hyperbolic Problems*. Cambridge University Press, 2002.
- [48] D. I. W. Levin, B. Gilles, B. Madler, and D. K. Pai, “Extracting skeletal muscle fiber fields from noisy diffusion tensor data,” *Medical Image Analysis*, vol. 15, pp. 340–353, 2011.
- [49] J. P. Lewis, M. Cordner, and N. Fong, “Pose space deformation: A unified approach to shape interpolation and skeleton-driven deformation,” in *SIGGRAPH '00: Proceedings of the Annual Conference on Computer Graphics and Interactive Techniques*, pp. 165–172, New York, NY, USA, 2000.
- [50] J. Lloyd, I. Stavness, and S. Fels, “The artisynth toolkit for rigid-deformable biomechanics,” in *ISB Technical Group on Computer Simulation Symposium, Poster*, June 2011.
- [51] Y.-Y. Ma, H. Zhang, and S.-W. Jiang, “Realistic modeling and animation of human body based on scanned data,” *Journal of Computer Science and Technology*, vol. 19, no. 4, pp. 529–537, 2004.
- [52] N. Magnenat-Thalmann, *Computer Animation: Theory and Practice*. New York, NY, USA: Springer-Verlag New York, Inc., 1985.
- [53] K. Min, S. Baek, G. Lee, H. Choi, and C. Park, “Anatomically-based modeling and animation of human upper limbs,” in *Proceedings of International Conference on Human Modeling and Animation*, 2000.
- [54] L. Moccozet and N. M. Thalmann, “Dirichlet free-form deformations and their application to hand simulation,” in *CA '97: Proceedings of the Computer Animation*, p. 93, Washington, DC, USA: IEEE Computer Society, 1997.
- [55] M. Mooney, “A theory of large elastic deformation,” *Journal of Applied Physics*, vol. 11, pp. 582–592, 1940.
- [56] A. Nealen, M. Mueller, R. Keiser, E. Boxerman, and M. Carlson, “Physically based deformable models in computer graphics,” *Computer Graphics Forum*, vol. 25, no. 4, pp. 809–836, December 2006.
- [57] L. P. Nedel and D. Thalmann, “Real time muscle deformations using mass-spring systems,” in *Proceedings of Computer Graphics International*, IEEE, 1998.
- [58] V. Ng-Thow-Hing, “Anatomically-based models for physical and geometric reconstruction of humans and other animals,” PhD Thesis, University of Toronto, Toronto, Canada, 2001.

- [59] V. Ng-Thow-Hing and E. Fiume, “B-spline solids as physical and geometric muscle models for musculoskeletal systems,” in *Proceedings of the International Symposium of Computer Simulation in Biomechanics*, pp. 68–71, 1999.
- [60] J. Nocedal and S. J. Wright, *Numerical Optimization*. Springer-Verlag, 2006.
- [61] C. W. J. Oomens, M. Maenhout, C. H. van Oijen, M. R. Drost, and F. P. Baaijens, “Finite element modelling of contracting skeletal muscle,” *Philosophical Transactions: Biological Sciences*, vol. 358, pp. 1453–1460, 2003.
- [62] D. K. Pai, “Muscle mass in musculoskeletal models,” *Journal of Biomechanics*, vol. 43, no. 11, pp. 2093–2098, 2010.
- [63] M. G. Pandy, F. E. Zajac, E. Sim, and W. S. Levine, “An optimal control model for maximum-height human jumping,” *Journal of biomechanics*, vol. 23, pp. 1185–1198, 1990.
- [64] S. I. Park and J. K. Hodgins, “Capturing and animating skin deformation in human motion,” *ACM Transactions on Graphics*, vol. 25, no. 3, pp. 881–889, 2006.
- [65] S. I. Park and J. K. Hodgins, “Data-driven modeling of skin and muscle deformation,” *ACM Transactions on Graphics*, vol. 27, no. 3, pp. 1–6, 2008.
- [66] W. H. Press, B. P. Flannery, S. A. Teukolsky, and W. T. Vetterling, *Numerical Recipes in C: The Art of Scientific Computing*. Cambridge University Press, 1992.
- [67] K. Ravichandiran, M. Ravichandiran, M. L. Oliver, K. S. Singh, N. H. McKee, and A. M. Agur, “Fibre bundle element method of determining physiological cross-sectional area from three-dimensional computer muscle models created from digitised fibre bundle data,” *Computer Methods and Programs Biomedical*, vol. 13, pp. 741–748, December 2010.
- [68] P. Sand, L. McMillan, and J. Popović, “Continuous capture of skin deformation,” *ACM Transactions on Graphics*, vol. 22, no. 3, pp. 578–586, 2003.
- [69] F. Scheepers, R. E. Parent, W. E. Carlson, and S. F. May, “Anatomy-based modeling of the human musculature,” in *SIGGRAPH Computer Graphics*, pp. 163–172, 1997.
- [70] T. W. Sederberg and S. R. Parry, “Free-form deformation of solid geometric models,” in *SIGGRAPH Computer Graphics*, pp. 151–160, 1986.
- [71] H. Seo and N. Magnenat-Thalmann, “An automatic modeling of human bodies from sizing parameters,” in *I3D '03: Proceedings of the 2003 symposium on Interactive 3D graphics*, pp. 19–26, New York, NY, USA: ACM, 2003.
- [72] K. Singh and E. Fiume, “Wires: a geometric deformation technique,” in *SIGGRAPH '98: Proceedings of the Annual Conference on Computer Graphics and Interactive Techniques*, pp. 405–414, New York, NY, USA, 1998.
- [73] P.-P. J. Sloan, C. F. Rose III, and M. F. Cohen, “Shape by example,” in *I3D '01: Proceedings of the 2001 Symposium on Interactive 3D Graphics*, pp. 135–143, New York, NY, USA: ACM, 2001.
- [74] I. Stavness, A. Hannam, J. Lloyd, and S. Fels, “Predicting muscle patterns for hemimandibulectomy models,” *Computer Methods in Biomechanics and Biomedical Engineering*, vol. 13, no. 4, 2010.
- [75] I. Stavness, J. Lloyd, Y. Payan, and S. Fels, “Coupled hardsoft tissue simulation with contact and constraints applied to jawtonguehyoid dynamics,”

- International Journal for Numerical Methods in Biomedical Engineering*, vol. 27, no. 3, 2011.
- [76] I. K. Stavness, “Byte your tongue: A computational model of human mandibular-lingual biomechanics for biomedical applications,” University of British Columbia, Vancouver, Canada, December 2010.
- [77] J. T. Stern, “Computer modelling of gross muscle dynamics,” *Journal of biomechanics*, vol. 7, no. 5, pp. 411–428, 1974.
- [78] G. Strang and G. Fix, *An Analysis of the Finite Element Method*. Wellesley-Cambridge, 2nd Edition, 2008.
- [79] S. Sueda, A. Kaufman, and D. K. Pai, “Musculotendon simulation for hand animation,” *ACM Transactions on Graphics*, vol. 27, no. 3, pp. 1–8, 2008.
- [80] C. Y. Tang, G. Zhang, and C. P. Tsui, “A 3D skeletal muscle model coupled with active contraction of muscle fibres and hyperelastic behaviour,” *Journal of biomechanics*, vol. 42, no. 7, pp. 865–872, 2009.
- [81] J. Teran, S. Blemker, V. N. T. Hing, and R. Fedkiw, “Finite volume methods for the simulation of skeletal muscle,” in *SCA '03: Proceedings of the 2003 ACM SIGGRAPH/Eurographics Symposium on Computer Animation*, pp. 68–74, 2003.
- [82] J. Teran, E. Sifakis, S. S. Blemker, V. Ng-Thow-Hing, C. Lau, and R. Fedkiw, “Creating and simulating skeletal muscle from the visible human data set,” *IEEE Transactions on Visualization and Computer Graphics*, vol. 11, no. 3, pp. 317–328, 2005.
- [83] D. Thalmann, J. Shen, and E. Chauvineau, “Fast realistic human body deformations for animation and VR applications,” in *CGI '96: Proceedings of the 1996 Conference on Computer Graphics International*, pp. 166–174, 1996.
- [84] W. Tsang, K. Singh, and E. Fiume, “Helping hand: An anatomically accurate inverse dynamics solution for unconstrained hand motion,” in *SCA '05: Proceedings of the 2005 ACM SIGGRAPH/Eurographics Symposium on Computer Animation*, pp. 319–328, 2005.
- [85] X. Tu and D. Terzopoulos, “Artificial fishes: Physics, locomotion, perception, behavior,” in *SIGGRAPH Computer Graphics*, pp. 43–50, 1994.
- [86] B. R. Umberger, K. G. M. Gerritsen, and P. E. Martin, “A model of human muscle energy expenditure,” *Computer Methods in Biomechanics and Biomedical Engineering*, vol. 6, no. 2, pp. 99–111, 2003.
- [87] A. J. van Soest and M. F. Bobbert, “The contribution of muscle properties in the control of explosive movements,” *Biological Cybernetics*, vol. 69, pp. 195–204, 1993.
- [88] D. R. Veronda and R. A. Westmann, “Mechanical characterization of skin-finite deformations,” *Journal of Biomechanics*, vol. 3, no. 1, pp. 111–124, 1970.
- [89] J. Wilhelms, “Animals with anatomy,” *IEEE Computer Graphics and Applications*, vol. 17, no. 3, pp. 22–30, 1997.
- [90] J. Wilhelms and A. Van Gelder, “Anatomically based modeling,” in *SIGGRAPH Computer Graphics*, pp. 173–180, 1997.
- [91] F. T. Wu, V. Ng-Thow-Hing, K. Singh, A. M. Agur, and N. H. McKee, “Computational representation of the aponeuroses as NURBS surfaces in 3D

- musculoskeletal models,” *Computer Methods and Programs in Biomedicine*, vol. 88, no. 2, pp. 112–122, 2007.
- [92] B. Wyvill and G. Wyvill, “Field functions for implicit surfaces,” *The Visual Computer*, vol. 5, no. 1–2, pp. 75–82, 1989.
- [93] C. A. Yucesoy, B. H. F. J. M. Koopman, P. A. Huijing, and H. J. Grootenboer, “Three-dimensional finite element modeling of skeletal muscle using a two-domain approach: Linked fiber-matrix mesh model,” *Journal of biomechanics*, vol. 35, no. 9, pp. 1253–1262, 2002.
- [94] G. I. Zahalak, “A distribution-moment approximation for kinetic theories of muscular contraction,” *Mathematical Biosciences*, vol. 55, no. 1–2, pp. 89–114, 1981.
- [95] F. E. Zajac, “Muscle and tendon: Properties, models, scaling, and application to biomechanics and motor control,” *Critical Review Biomedicine Engineering*, vol. 17, no. 4, pp. 359–411, 1989.
- [96] F. E. Zajac and M. E. Gordon, “Determining muscle’s force and action in multi-articular movement,” *Exercise and Sport Sciences Reviews*, vol. 17, pp. 187–230, 1989.
- [97] Q.-H. Zhu, Y. Chen, and A. Kaufman, “Real-time biomechanically-based muscle volume deformation using FEM,” *Computer Graphics Forum*, vol. 17, no. 3, pp. 275–284, December 2001.
- [98] V. B. Zordan, B. Celly, B. Chiu, and P. C. DiLorenzo, “Breathe easy: Model and control of human respiration for computer animation,” *Graphical Models*, vol. 68, no. 2, pp. 113–132, 2006.